Limit Analysis Under the Aspect of Catastrophe Theory

F.G. Rammerstorfer, D.F. Fischer
Voest-Alpine AG, Postfach 2, A-4010 Linz, Austria

The catastrophe theory, originally introduced to deal with jump phenomena in biology in a mathematical manner, was recently intoduced into the field of structural mechanics, especially to explain and classify jump behaviour of statically loaded (stability) or dynamically loaded (nonlinear vibrations) structures.

The paper deals with the calculation of the stability limit load of nonlinear structures using the finite element technique. It is shown that some structures behaves catastrophically in a double sense, i.e. the load displacement behaviour shows catastrophic states indicated by snap-through buckling and, in addition, the stability limit load itself has a catastrophic parameter sensitivity. The latter means, that a small variation of a certain structural parameter (or a combination of parameters) may lead to a sudden jump of the stability limit load. This has, of course, crucial consequences for safety considerations of such structures with respect to their stability limit load, particularely concerning the accuracy and tolerances of significant system parameters. Consider for example the already earlier investigated circular arch elastically restrained at its ends. For this structure the stiffness of the support restraints is such a significant system parameter for which an infinitely small variation may render a sudden non-continuous decrease of the stability limit load. Further technical relevant structures will be investigated in the paper.

The stability analyses were performed by considering the behaviour of the current tangent stiffness matrix of the structure as well as by accompanying eigenvalue analyses.

Catastrophic behaviour regarding the stability limit is indicated if the determinant vanishes but does not change its sign at that load level. A special generalized potential function governs the catastrophe of jumping limit loads.

1. Introduction

Considering the load displacement behaviour in combination with the variation of the determinant of the global tangent stiffness matrix and performing supplementary eigenvalue-analyses at several load steps, the stability behaviour of nonlinear structures can be determined. Some unexpected effects which a linear analysis would never reveal are found by those nonlinear investigations.

As shown by the authors in ref. [1] some structures can undergo effects like a non-continuous parameter sensitivity. This means that an infinitesimal variation of a particular parameter of the physical system can cause a sudden jump of the stability limit. It is shown how those problems are embedded in the catastrophe theory.

2. A short introduction to the catastrophe theory

The rather young mathematical theory of catastrophes has its origin in the endeavour to render mathematical models of natural processes having a certain jump behaviour, especially of such belonging to the field of biology, see Thom [2]. In the meantime this theory has found useful application in a wide variety of other fields as shown by Thom [3] and Zeeman [4]. Troger [5,6] used this theory to classify phenomena concerning the stability of the equilibrium of mechanical structures.

Consider a mechanical system which has a parameter dependent behaviour. Points in the parameter domain at which the system changes its behaviour in a qualitative sense due to a variation of the parameters (a, b) are called bifurcation points. Assume for simplicity that the system has a real scalar potential function, $V(x,a,b)$, e.g. the complete potential energy of a loaded elastic structure, with x the dependent variable, describing the state of the system, and a and b the independent system parameters (control parameters). The surface in the a, b, x domain which is defined by

$$\frac{\partial V}{\partial x} = 0 \tag{1}$$

represents the behaviour surface, e.g. the equilibrium states of the elastic structure. The parameter domain is in this case the plane a - b and is named the control surface. The system is structurally stable if a small variation of the system parameters does not change the qualitative character of the potential function, otherwise the system is structurally unstable [6]. Applying the more general classification theorem of R. Thom [2] to this special case the following statement holds: The behaviour surface is - provided the system is structurally stable - a smooth surface, whose projection into the parameter domain (control surface) has only fold curves and cusps, see fig. 1. The fold curves are the set of the bifurcation points $(a,b)^*$ in the control surface for which the condition

$$\left.\frac{\partial^2 V}{\partial x^2}\right|_{(a,b)^*} = 0 \tag{2}$$

is met, e.g. snap-through conditions for the elastic structure.

In the considered special case the potential, $V(x;a,b)$, can be described in the vicinity of the cusp qualitatively by one of the following polynomials [2,6]:

$$V = \frac{1}{3}x^3 + ax \quad \text{or} \quad V = \frac{1}{4}x^4 + \frac{1}{2}ax^2 + bx \tag{3, 4}$$

In case of eq. (4) the behaviour surface is defined by eq. (1) which renders now:

$$\frac{\partial V}{\partial x} = x^3 + ax + b = 0 \tag{5}$$

Application of eq. (2) and elimination of x yields under consideration of eq. (5) the bifurcation set in the control surface:

$$4a^3 + 27b^2 = 0, \tag{6}$$

which represents parabolas forming a cusp.

Catastrophes defined by a potential corresponding to eq. (4) belong to the class of cusp catastrophes.

A simple example taken from [6], the v. Mises truss, may demonstrate the statements given above. Figure 1 shows the behaviour surface of this structure. For this example the potential is given by [6]:

$$V = \frac{1}{4}\alpha^4 - \frac{\alpha_o^2}{2}\alpha^2 + \frac{P}{EA}\alpha + \left(\frac{\alpha_o^4}{4} - \frac{P}{EA}\alpha_o\right) \tag{7}$$

In order to correspond with eqs. (3 - 6) the following quantities must be introduced:

$$x = \alpha, \quad a = -\alpha_o^2, \quad b = P/EA \tag{8}$$

Thus, the catastrophic behaviour of the v. Mises truss is described by the eqs. (5 and 6) concerning equilibrium states and stability limits, respectively. The shaded area in fig. 1 is limited by the fold curves; it has the following significance: If a parameter value crosses one of the fold curves coming from the shaded area, then a continuous parameter variation renders a non-continuous system behaviour, i.e. snap-through.

3. Application of the catastrophe theory to particular practical problems

3.1 An elastically supported circular arch

Consider the circular arch, elastically restrained at both ends, in fig. 2 which was investigated in detail by the authors [1]. This simple structure represents a highly nonlinear system and has a very interesting stability behaviour.

The real background for the choice of this structure as an example is the consideration of the nonlinear behaviour of wide spanned roofs of very large storage tanks. The stiffness coefficients c_1 and γ of the restraining springs are varied in order to calculate the sensitivity of the structure with regard to this variation:

$$c_1 = C\, c_{1ref}, \quad \gamma = \Gamma\, \gamma_{ref}, \tag{9}$$

C and Γ are used as restraint parameters.

Proportional load is assumed, i.e. the load vector $\underset{\sim}{R}$ is given by

$$\underset{\sim}{R} = \lambda\, \underset{\sim}{R}_{ref} \tag{10}$$

with $\underset{\sim}{R}_{ref}$ the reference load vector and λ the load multiplier.

The distributed load is location dependent:

$$q(r) = q_o \frac{r}{r_s} \tag{11}$$

with $q_o = 5.04 \times 10^4$ N/m at load level $\lambda = 1$.

Only displacements in the y-z-plane are allowed (plane problem).

Fig. 3 shows the results of the nonlinear incremental-iterative analysis [1]. The case with $C = 1$, $\Gamma = 1$ is considered. The motion of the support K which represents the motion of the central ring of the tank roof during load incrementation is remarkable. At the beginning of the load incrementation it moves upwards and after reaching a limit it moves downwards until the arch snaps through. This peculiar behaviour of the support motion is also reflected in the curious load dependence of the normal compression force $N(\lambda)$ which causes the alternating stiffness variation represented by the $\det_n \underset{\approx}{K}(\lambda)$ history. $\det_n \underset{\approx}{K}(\lambda)$ is the normalized determinant of the global tangent stiffness matrix $\underset{\approx}{K}$ at load level λ. Considering the eigenvalue functions, $\lambda^*(u)$, which represents approximative values of the critical load level, λ^*, resulting from accompanying eigenvalue analyses corresponding to ref. [1], and the $\det_n \underset{\approx}{K}(\lambda)$ curve one gets the impression that the structure is almost at a stability limit at $\lambda \approx 1.4$ (the $\det_n \underset{\approx}{K}(\lambda)$ curve approaches the λ axis and the $\tilde{\lambda}^*$ curves tend to touch the $\lambda(u)$ paths) but a further load incrementation "stiffens" the structure until $\lambda \approx 2.5$. Continuation of the load incrementation leads finally to the snap-through buckling at $\lambda \approx 3$: The $\det_n \underset{\approx}{K}(\lambda)$ curve reaches a limit with horizontal tangent and the $\lambda^*(u)$ curves cross the load displacement paths. Special attention will now be given to the $\det_n \underset{\approx}{K}(\lambda)$ history. It is obvious that after a certain parameter variation the $\det_n \underset{\approx}{K}(\lambda)$ curve may cross the λ axis just before the "re-stiffening period". This would render a sudden change of the critical load level, λ^*.

3.1.1 Parameter sensitivity

In order to find a sensitivity behaviour as presumed in the previous chapter the spring stiffness c_1, expressed by C according to eq. (9) is varied.
Figure 4 shows the results of three typical cases:

a) $C = 1.0$: Load incrementation leads to a stiffness-loss followed by a re-stiffening, a further stiffness-loss and finally the snap-through.
b) $C = 0.5$: It is remarkable that the determinant curve crosses the λ axis before re-stiffening takes place. Considering the $\lambda(u^K)$ behaviour one can observe that the support K snaps upwards quite contrary to the case $C = 1$ in which it snaps downwards. This value of C is already beyond the critical value of $C = C^*$ at which the limit load jumps (see also fig. 5).
c) $C = 0.35$: The system moves towards the snap-through in a direct manner just like the usual hinged-hinged arch.

Further variation of the parameter C allows the presentation of the parameter sensitivity of the limit load, $\lambda^*(C)$, in fig. 5 which clearly shows the considerable jump of $\lambda^*(C)$ at $C = C^* \approx 0.55$. This jump behaviour has of course serious consequences for the design of such structures and the criticism concerning their stability safety.

3.1.2 Embedding in the catastrophe theory

Systems like the considered one have catastrophic behaviour in a double sense: Firstly, the load displacement behaviour shows catastrophic states indicated by snap-through at $\lambda = \lambda^*$ and, secondly, the stability limit load itself has a catastrophic parameter sensitivity.

Let us choose the load multiplier, λ, and the restraining parameter, C, as independent control parameters and the vertical displacement, u_z^K, of the support K as dependent behaviour variable.

The results of the above described analysis render the behaviour surface, $-u_z^K(\lambda, C)$, as shown qualitatively in fig. 6. The potential, V, describing this behaviour is, naturally, the total potential energy. To emphasize the different character of the two domains of the behaviour surface in fig. 6 a cut is made along the line $C = C^*$: For $C < C^*$ the point K (central ring of the roof) snaps through upwards, for $C > C^*$ downwards.

This behaviour surface, $-u_z^K(\lambda, C)$, describes the first catastrophic aspect. A second one is the non-continuous variation of the stability limit load for some parameter variation. Figure 7 shows schematically the dependence of the critical load multiplier, $\lambda = \lambda^*$, on the system parameters (control parameters) C and Γ. It will be shown by the relevant potential that we again are dealing with a cusp catastrophe.

In fig. 7 the behaviour surface, $\lambda^*(C,\Gamma)$, is shown for $\Gamma \leqslant 1$. The cross section at $\Gamma = 1$ corresponds with the $\lambda^*(C)$ curve in fig. 5. Furthermore, some points on the behaviour surface for $C = 1.0$, i.e. $\lambda^*(\Gamma, C=1)$ are calculated. From these informations the behaviour surface was drawn qualitatively.

The potential $\tilde{V}$ belonging to this catastrophic behaviour is obtained by

$$\tilde{V}(s(\bar{\lambda})) = - \oint_0^{s(\bar{\lambda})} \det_{\tilde{n}} K(\lambda) ds + D \tag{12}$$

with $s(\bar{\lambda})$ being the arc length of the $\det_{\tilde{n}} K(\lambda)$ curve from $\lambda = 0$ to $\lambda = \bar{\lambda}$. (Since $\det_{\tilde{n}} K(\lambda)$ is not in general an unique function a parameter representation by the mapping $\lambda \longrightarrow s(\lambda)$ is necessary.) D is an arbitrary real constant.

$$\left.\frac{\partial \tilde{V}}{\partial s}\right|_{\lambda=\lambda^*} = 0 \quad \text{and} \quad \left.\frac{\partial^2 \tilde{V}}{\partial s^2}\right|_{\lambda=\lambda^*,\ C=C^*(\Gamma)} = 0 \tag{13,14}$$

render with the necessary condition [1] (15)

$$\left.\det_{\tilde{n}} K\right|_{\lambda=\lambda^*} = 0$$

and by applying the inverse mapping, $s^{-1}(\lambda) \Longrightarrow \lambda$, the behaviour surface and the bifurcation set, $C^*(\Gamma)$.

The condition for the jump of $s(\lambda^*)$, eq.(14), leads in combination with eq. (15) to that situation in which the $\det_{\tilde{n}} K(\lambda)$ curve touches the λ axis without crossing it. This is exactly the case if C approaches C^*.

The potential $\tilde{V}$, schematically shown in fig. 8 for $C < C^*$, $C = C^*$ and $C > C^*$, behaves like a polynomial with order four which is in correspondence with eq. (4). Referring to Thom's theorem one can conclude that the assumption of a cusp catastrophe is justified. For values $C > C^*$ a point of inflection in the $\tilde{V}(s(\lambda))$ curve exists at a $\lambda < \lambda^*$ but only one minimum of $\tilde{V}$ subsists. The appearance of a second minimum of $\tilde{V}$ for $C < C^*$ renders the jump of $\lambda^*(C)$ at $C = C^*$.

3.2 The shallow spherical cap

As a further example consider the shallow spherical segment in fig. 9. Axisymmetric conditions and proportional pressure load, $p = \lambda p_{ref}$, are assumed. In this example the radius relation $\rho = R/R_{ref}$ and the load multiplier, λ, are found to act as independent control parameters. The downward displacement of the top, u_M, is the dependent variable. Figure 10 shows the load displacement paths, i.e. $\lambda(u_M)$ curves, for different ρ-values. Typical snap-through buckling is observed. However, for $\rho > \rho^*(\approx 2.4)$ no buckling appears. This renders a behaviour surface similar to that of the v. Mises truss previously discussed; a cusp catastrophe is derived.

In fig. 11 the $\det_n \underset{\approx}{K}(\lambda)$ curves and the relation between the force in the support spring and λ, i.e. $N(\lambda)$, are shown for ρ values near the critical value ρ^*, the cusp of the bifurcation set, see fig. 10. We observe an effect similar to that discussed in fig. 8 for the arch example: For $\rho > \rho^*$ the $\det_n \underset{\approx}{K}(\lambda)$ curve approaches the λ-axis but does not cross or touch it. For $\rho = \rho^*$ the λ-axis is touched by $\det_n \underset{\approx}{K}$ and for $\rho \leqslant \rho^*$ we find $\det_n \underset{\approx}{K}(\lambda)$ curves typical for snap-through buckling. Hence in the vicinity of ρ^* also this structure has a non-continuous parameter sensitivity: For $\rho > \rho^*$ a slow increase of the pressure load leads to a quasi static response (axisymmetry assumed), however for $\rho \leqslant \rho^*$ and $\lambda > \lambda^*(\rho)$ dynamic effects appear despite a careful pressure increase.

4. Conclusions

The paper shows catastrophic behaviour of structures in a double sense: a sudden change of the equilibrium configuration and jumps of the stability limit load. In ref. [1] criteria are given which allow a classification of structures with respect of the parameter sensitivity of the stability limit load - continuous or not.

References

[1] RAMMERSTORFER, F.G., FISCHER, D.F., "Parameter Sensitivity of Nonlinear Structures Concerning Stability Limit", Proceedings Europe - U.S. Workshop Nonlinear Finite Element Analysis in Structural Mechanics, Bochum, Germany, July 28 - 31, 1980, in press by Springer-Verlag.

[2] THOM, R., "Topological Models in Biology", Topology 8, pp. 313 - 335 (1969).

[3] THOM, R., "Structural Stability and Morphogenesis", New York: Benjamin 1975.

[4] ZEEMAN, E.C., "Catastrophe Theory", Scientific American, April 1976, pp. 65 - 83.

[5] TROGER, H.: "Zur Einteilung von Sprungeffekten in mechanischen Systemen", ZAMM 54, pp. T177 - T179 (1974).

[6] TROGER, H.: "Ein Beitrag zum Durchschlagen einfacher Strukturen", Acta Mechanica 23, pp. 179 - 191 (1975).

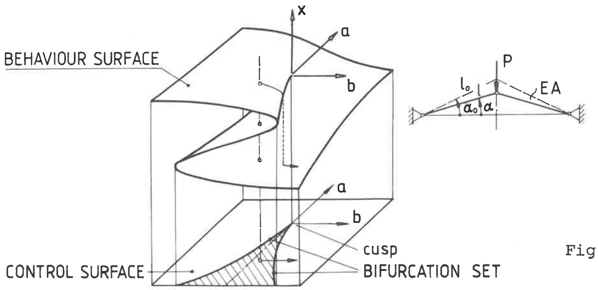

Fig. 1: The behaviour surface and the bifurcation set - v. Mises truss.

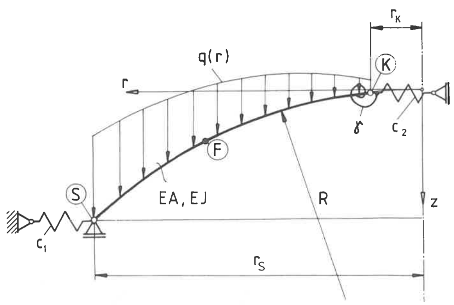

Fig. 2: The circular arch

$R = 105$ m, $r_x = 1.92$ m, $r_s = 34.6$ m,
$EA = 1.74 \times 10^9$ N, $EJ = 2.71 \times 10^7$ Nm^2,
$c_{1ref} = 1.4 \times 10^7$ N/m, $c_2 = 6 \times 10^8$ N/m,
$\gamma_{ref} = 2.7 \times 10^7$ Nm/rad.

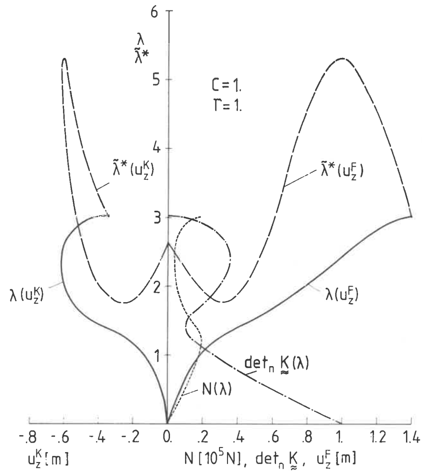

Fig. 3: The nonlinear behaviour of the arch ($C = 1$, $\Gamma = 1$).

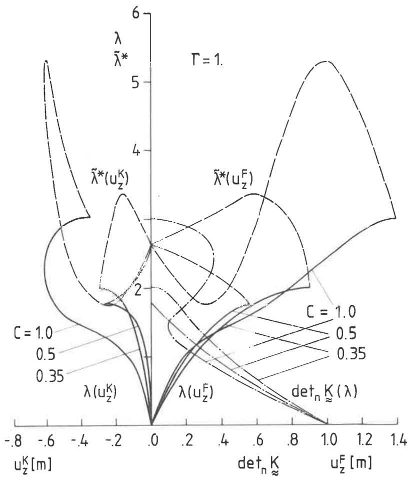

Fig. 4: Behaviour of the arch with different spring stiffness, C.

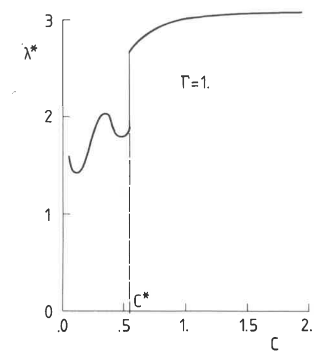

Fig. 5: Stability limit load, $\lambda^*(C;\Gamma=1)$.

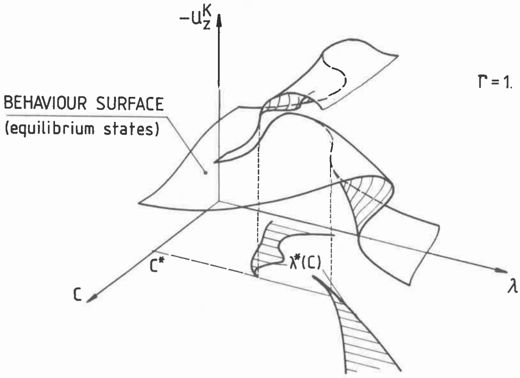

Fig. 6: The behaviour surface of the arch with regard to equilibrium states.

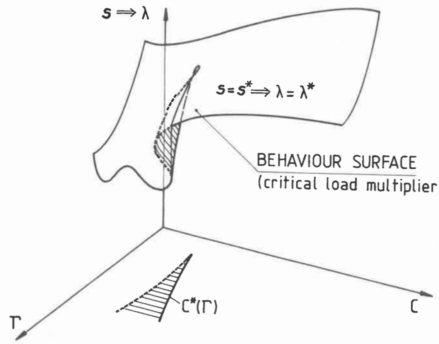

Fig. 7: The catastrophic behaviour of the critical load level.

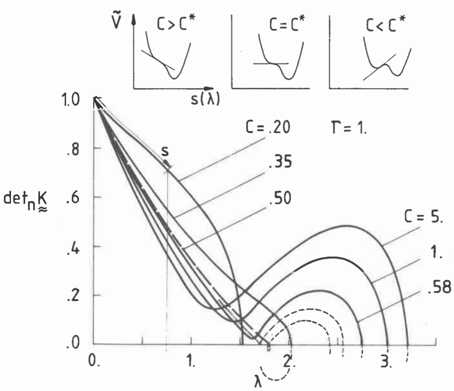

Fig. 8: The normalized determinant and the corresponding potential $\tilde{V}$ (thin dotted lines are expected).

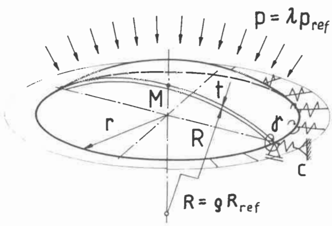

Fig. 9: The spherical cap

R_{ref} = 10 m, r = 1 m, t = 5 mm,

c = 2.1 x 10^{12} (N/m)/rad,

γ = 4 x 10^{5} (Nm/rad)/rad,

p_{ref} = 50 kN/m^2.

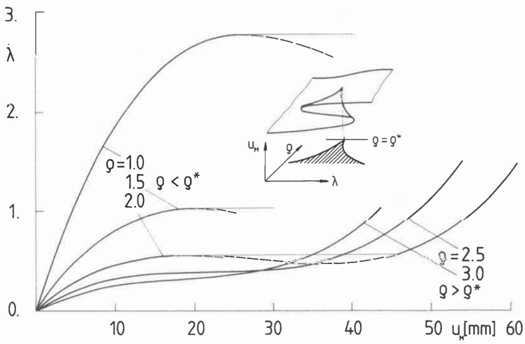

Fig. 10: The load displacement path for different cap curvatures; behaviour surface.

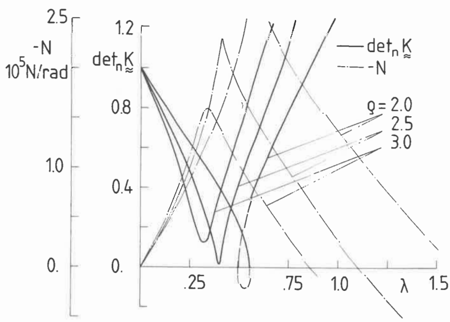

Fig. 11: Normalized determinant and spring force for different cap curvatures.